

Characterization of $\text{CaSn}(\text{OH})_6$ and CaSnO_3 Nanostructures Synthesized by a New Precursor

S. Moshtaghi^a, D. Ghanbari^b, M. Salavati-Niasari^{a*}

^a Institute of Nano Science and Nano Technology, University of Kashan, Kashan, P.O. Box, 87317-51167, I. R. Iran.

^b Young Researchers and Elite Club, Arak Branch, Islamic Azad University, Arak, Iran

Article history:

Received 11/04/2015

Accepted 27/05/2015

Published online 01/06/2015

Keywords:

CaSnO_3

Nanoparticles

Photo-catalyst

*Corresponding author:

E-mail address:

Salavati@kashanu.ac.ir

Phone: +98 361 591 2383

Fax: +98 361 555 29 30

Abstract

In this paper, calcium stannate nanoparticles were synthesized by a fast and simple co-precipitation procedure. For CaSnO_3 preparation ammonia was used as precipitation agent. The effect of various surfactants such as cationic, anionic and neutral on the morphology of the products was investigated. By changing in $\text{Ca}(\text{Sal})_2$ as a new precursor different morphologies were obtained. Ligand as a capping agent with steric hindrance leads to preparation of product with lower particle size. These semiconductor nanostructures have photo-catalyst activities and can degrade organic dyes as water pollution. The synthesized materials were characterized by X-ray diffraction (XRD) technique, scanning electron microscopy (SEM) Fourier transform infrared (FT-IR) and UV-visible spectroscopy.

2015 JNS All rights reserved

1. Introduction

Alkaline earth stannate (general formulae: ASnO) have very interesting properties, they have been receiving much attention for different applications such as components of ceramic dielectric materials, thermally capable capacitors and semiconducting sensors for gases. CaSnO_3 as n-type semiconductor because of wide-energy-gap (4.3 eV) attracted many consideration, therefore this product have used in many fields such as

transparent conducting films, catalytic materials, environmental monitoring, biochemical sensor, lithium rechargeable batteries and dye-sensitized solar cells [1-4]. ASnO_3 (A= Ba, Sr and Ca) have attracted technological interest due to their applications as transparent conducting oxides (TCOs), which are employed in the fabrication of transparent electrodes for photovoltaic cells and organic light-emitting diodes. ASnO_3 materials also have been used to develop new stable

capacitors, water photo-electrolysis systems, anti-static coatings and flat panel displays.

Due to this fact that oxygen atoms absorbed on the surface of the metal oxide, particle influences its electrical properties by producing an electron-depleted space-charge layer in the space-charge region of the species. These stannates have also been studied for their potential applications as sensor materials for host of gases, including CO, CH₄, H₂, Cl₂, NO [1-8]. The photocatalytic properties of semiconductor-based catalysts for producing clean H₂ fuel from water and degrading organic pollutants have received considerable attention, as energy and environmental concerns have given new impetus to solar-to-chemical conversion processes. It has been clearly shown that many organic and inorganic pollutants present in water or air can be completely decomposed by means of photocatalysis. The crystal structure of CaSnO is constructed of octahedral SnO₆, and these octahedra connect to each other by sharing vertexes. A network of corner-shared octahedra can facilitate the mobility of the charged carriers, which may make CaSnO₃ a novel material for photo-catalysis [5-12].

In this study, we synthesized CaSn(OH)₆ and CaSnO₃ by a simple and low-cost co-precipitation method using Ca(sal)₂ as a new precursor. The influence of different surfactants such as cationic, anionic and neutral on the morphology of the products was examined. By changing in Ca(sal)₂ and precursors different morphologies were obtained.

2 Experimental

2.1 Materials and characterization

All chemicals material were of analytical grade, SnCl₂, ammonia (NH₃), N(Et)₃,

Salicylaldehyde and Ca(NO₃)₂ · 4H₂O were purchased from Merck Company, and were used without further purification. XRD patterns were recorded by a Philips, X-ray diffractometer using Ni-filtered Cu K α radiation. FT-IR spectra were recorded on Galaxy series FTIR5000 spectrophotometer. Room temperature photoluminescence was studied by a Perkin Elmer fluorescence instrument. SEM images were obtained using a LEO instrument model 1455VP. Prior to taking images, the samples were coated with a very thin layer of Au to make the sample surface conductor and prevent charge accumulation, and obtaining a better contrast.

2.2. Synthesis of [bis(salicylaldehydato)calcium (II)]; Ca(sal)₂

4 g of Ca(NO₃)₂ · 4H₂O was dissolved in 60 mL distilled water in 60 °C under magnetic stirring. 3.55 mL of salicylaldehyde was dissolved in 40 mL methanol in 60 °C. After that 4.5 mL of N(Et)₃ was added to salicylaldehyde solution under magnetic stirring drop by drop. Then this solution was added drop wise to the calcium solution. The organometallic precursor was separated as white powder and was recrystallized twice from methanol (yield 90%). In final, the resulting precipitate was dried at 70 °C.

2.3. Synthesis of CaSn(OH)₆ and CaSnO₃

CaSn(OH)₆ was prepared via precipitation method. Appropriate amounts of Ca(sal)₂ and SnCl₂ were used as the calcium and tin precursors. In a typical synthesis Ca(sal)₂ was dissolved in 40 mL distilled water and SnCl₂ was dissolved in 30 mL distilled water. Then Ca(sal)₂ was heated at 60 °C for 5 min and finally the SnCl₂ solution was added drop wise to this solution. Finally ammonia was added to this solution drop by drop to achieved pH = 13. Solution was heated at 60 °C for 60 min under stirring. CaSn(OH)₆ was filtered, washed

with distilled water and ethanol several times and dried in vacuum in less than 80 °C. After that dried product was heated at 900 °C in air for 5 hour .

3. Results and discussion

XRD pattern of $\text{CaSn}(\text{OH})_6$ is shown in Fig. 1 which is indexed as a cubic phase (space group: Pn-3). The experimental values are very close to the literature (JCPDS No. 74-1823).

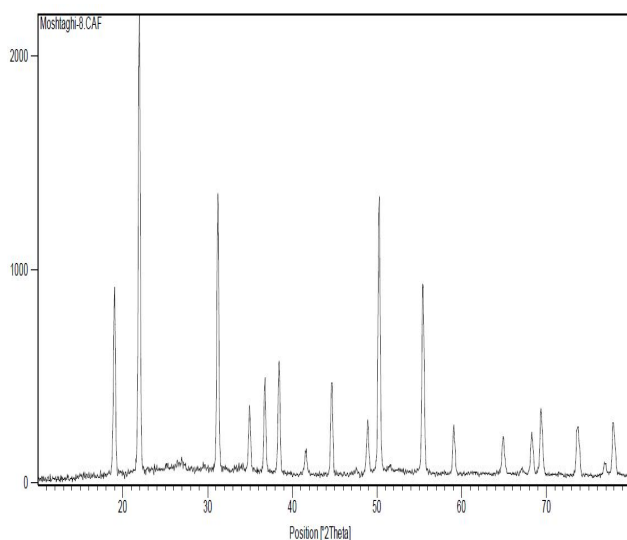


Fig. 1. XRD pattern of $\text{CaSn}(\text{OH})_6$

XRD pattern of CaSnO_3 is illustrated in Fig 2 .which is indexed as a orthorhombic phase (space group: Pn212121). The experimental values are very close to the literature (JCPDS No. 31-0312).

The crystallite size measurements were carried out using the Scherrer equation: $D_c = 0.9\lambda / \beta \cos\theta$ where β is the width at half maximum intensity of the observed diffraction peak, and λ is the X-ray wavelength (CuK_α radiation, 0.154 nm). The estimated crystallite size is about 37 nm.

SEM image of CaSnO_3 obtained by surfactant-free reaction and using ammonia as precipitating agent is illustrated in Fig 3. By using ammonia agglomerated nanoparticles were synthesized however mediocre size of calcium stannate is less than 100 nm.

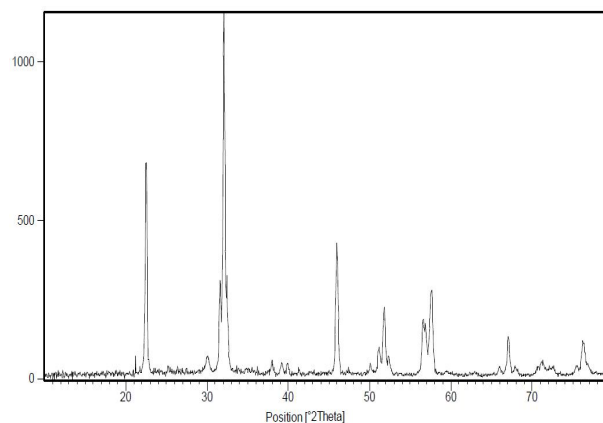


Fig. 2. XRD pattern of CaSnO_3

The effect of various surfactants such as cationic, anionic and neutral on the morphology of the products was investigated.

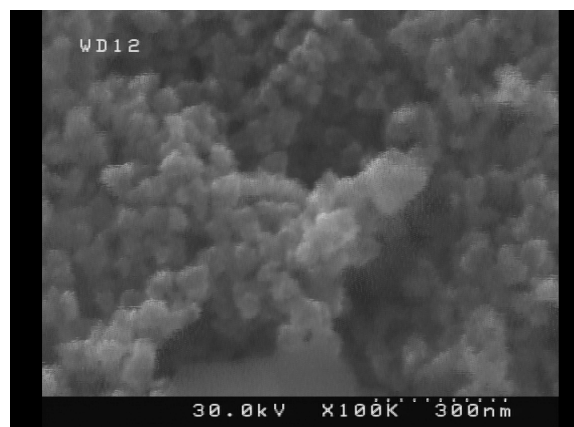


Fig. 3. SEM of surfactant-free product

By using cetyl tri-methyl ammonium bromide (CTAB as a cationic surfactant), sodium dodecyl sulfonate (SDS as an anionic surfactant) and poly ethylene glycol (PEG 4000 as neutral capping agent) the morphology of nanoparticles was changed. Fig 4 shows synthesized product with CTAB. Fig 5 illustrates CaSnO_3 nanoparticles obtained with PEG 4000.

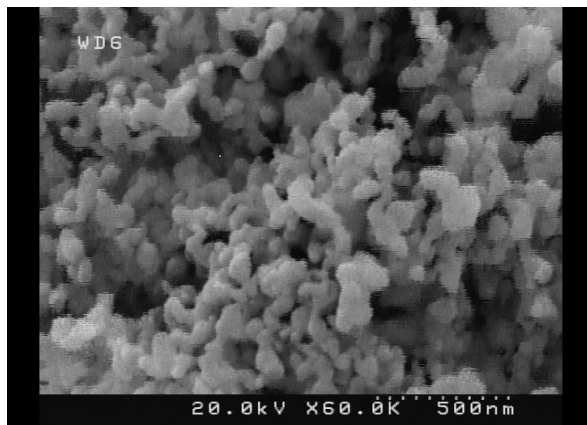


Fig. 4. SEM image of CaSnO_3 with CTAB

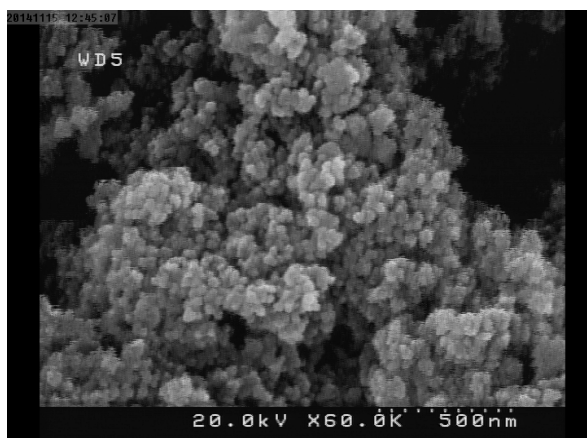


Fig. 5. SEM image of CaSnO_3 with PEG

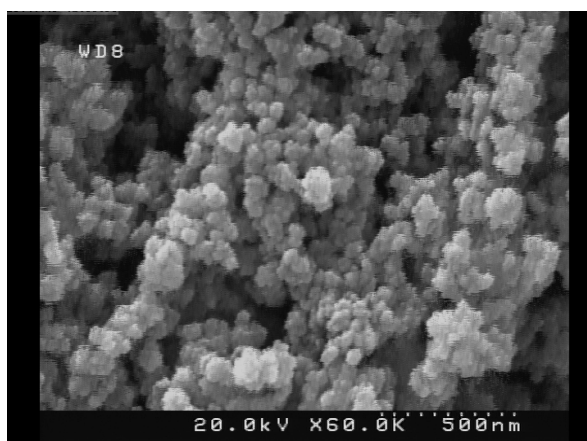


Fig. 6 SEM image of CaSnO_3 with SDS

Average particle size of all nanoparticles are less than 100 nm and results also confirm that by using SDS and CTAB mono-dispersed nanoparticles with

lower agglomeration were synthesized. Fig 6 exhibits the nanoparticles achieved by SDS.

UV-visible absorption spectrum of CaSnO_3 nanoparticles is illustrated in Fig.7. FT-IR absorption spectrum of CaSn(OH)_6 is depicted in Fig.8. Absorption around 400-600 and peak at 3230 cm^{-1} are responsible to Sn-O and O-H of CaSn(OH)_6 respectively. Broad peak at 3250-3500 is responsible for hydroxyl adsorbed on the surface of nanoparticles. FT-IR absorption spectrum of CaSnO_3 is shown in Fig.9. Absorption around $400\text{--}600\text{ cm}^{-1}$ is related to Sn-O bonds and broad peak at $3300\text{--}3500\text{ cm}^{-1}$ is responsible for hydroxyl adsorbed on the surface of CaSnO_3 nanoparticles.

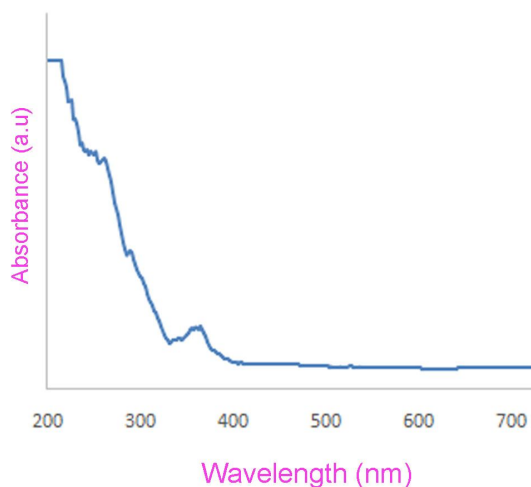


Fig. 7. UV absorption spectrum of CaSnO_3

Acid brown 14 and acid blue 92 as typical organic pollutants were employed as targets because of the relative stability of their molecular structure. The as-prepared nanoparticles have the potential to be applied to improve environmental problems associated with organic and toxic water pollutants. The photo-catalytic activity of the nanoparticles was evaluated by monitoring the degradation of organic dyes in an aqueous solution, under irradiation with UV light.

As time increased, more and more dye is adsorbed on the nanoparticles catalyst, until the absorption peaks (λ_{max}) of acid brown 14 and acid blue 92 that are 416 and 571 nm respectively, decrease and vanish around 120 min [13]. dyes were degraded at 120 min of irradiation. The dyes concentration decreased rapidly with increasing UV-irradiation time, and the absorption peaks almost disappeared after 120 min.

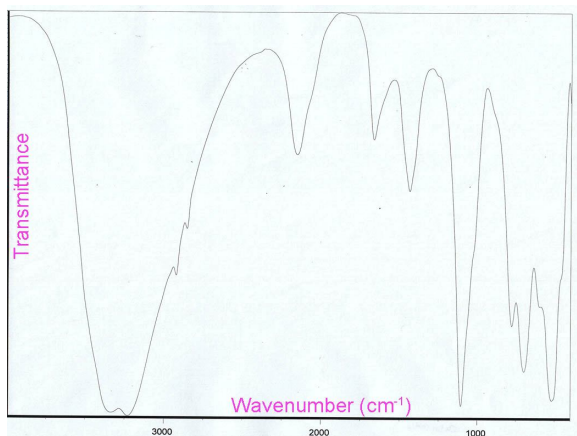


Fig. 8. FT-IR spectrum of $\text{CaSn}(\text{OH})_6$

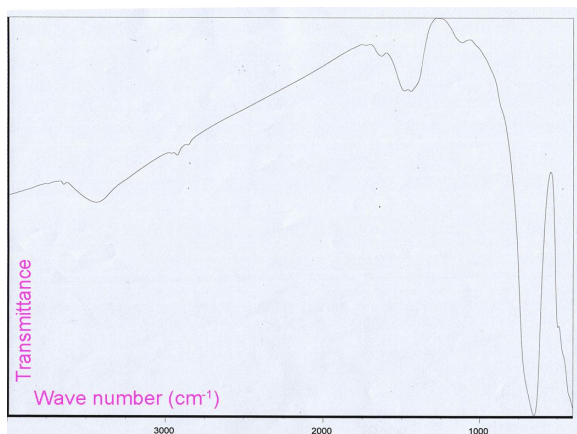


Fig. 9. FT-IR spectrum of CaSnO_3 nanoparticles

4. Conclusion

Different structures of calcium stannate nanostructures were synthesized via chemical reaction, the influence of various precursors and surfactants on the particle sized of the products

was investigated. Photo-catalytic property of CaSnO_3 in degradation as acid brown 14 and acid blue 92 as organic pollutants in water was investigated. Nanostructures were characterized by XRD, SEM, and FT-IR.

Acknowledgment

The authors are grateful to council of University of Kashan for providing financial support to undertake this work.

References

- [1] X. Hu, T. Xiao, W. Huang, W. Tao, B. Heng, X. Chen, Y. Tang Appl Surf Sci 258 (2012) 6177–6183
- [2] J. Ahmed, C. K. Blakely, S. R. Bruno, V.V. Poltavets Mater Research Bulletin 47 (2012) 2282–2287
- [3] A.S. Deepa, S. Vidya, P.C. Manu, Sam Solomon, Annamma John, J.K. Thomas. J Alloy Compd 509 (2011) 1830–1835
- [4] P. Junploy, S. Thongtem, T. Thongtem, Superlatt Microstruc 57 (2013) 1–10
- [5] W. Wang, J. Bi, Ling Wu, Z. Li, X. Fu, Scripta Materialia 60 (2009) 186–189
- [6] Y. Wang, Ch. Ma, X. Sun, H. Li, Inorg. Chem. Commun.5 (2002) 751-755.
- [7] C. Guo, M. Cao, Ch. Hu, Inorg. Chem. Commun. 7 (2004) 929–931.
- [8] H.R. Momenian, S. Gholamrezaei, M. Salavati-Niasari, B. Pedram, F. Mozaffar, D. Ghanbari, J Clust Sci 24 (2013) 1031-1042
- [9] D. Ghanbari, M. Salavati-Niasari M. Ghasemi-Kooch. J Ind Eng Chem. 20 (2014) 3970-3974 .
- [10] E. Callone, G. Carturan, M. Ischia, M. Epifani, A. Forleo, P. Siciliano, R. Paolesse, Inorg. Chim. Acta 361 (2008) 79-85.
- [11] O. Lupana, L. Chowa, G. Chaic, A. Schultea, S. Parka, H. Heinricha, Mater. Sci. Eng., B 157

(2009) 101-104.

[12] S. Zhang, B. Yin, Y. Jiao, Y. Liu, F. Qu, X. Wu, *Appl. Surf. Sci.* 305 (2014) 626-629.

[13] L. Nejati Moghadam, A. Esmaili-Bafghi M. Salavati-Niasari H. Safardoust. *J Nano Struc.* 5 (2015) 47-53